Deformation behaviour of an amorphous Fe-Ni-W/Ni bilayer confined bulk metallic glasses

H.Q. Lau, Natalie Yip, S.H. Chen, W. Chen, K.C. Chan*

Advanced Manufacturing Technology Research Centre, Department of Industrial and Systems Engineering, The Hong Kong Polytechnic University, Hong Kong.

* Corresponding author. Tel.: +852 27664981. E-mail address: kc.chan@polyu.edu.hk (K.C. Chan).

Abstract

In this study, an amorphous Fe-Ni-W/Ni bilayer has been successfully electroplated on a Zr-based bulk metallic glass (BMG), and the deformation behaviour of the bilayer coating confined BMG has been investigated. The findings show that the macroscopic plasticity of the BMGs has been enhanced from 1.3% to 10.7%. More importantly, bilayer confined BMGs have a large plateau of serrated flow with insignificant decrement before failure. When characterizing the serrated flow of both uncoated and bilayer confined BMGs by introducing an absolute value of the stress raises/drops, smaller amplitudes of stress drops as well as larger stress drop frequency during the plastic deformation stage has been found in the bilayer confined BMGs. The origin of the increased stable plastic flow has been discussed, and is mainly attributed to the enhanced confinement caused by introducing the amorphous layer. The findings are of significance in enhancing the macroscopic plasticity of BMGs and in understanding the deformation mechanism of serrated plastic flow in geometrical confined BMGs.

Keywords: Plastic flow; Bulk metallic glass; Amorphous Fe-Ni-W coating; Geometric confinement.

1. Introduction

In recent years, due to the extraordinary mechanical properties of bulk metallic glasses (BMGs), such as high strength and high elastic strain, there has been a growing interest in exploring the application potential of BMGs as structural materials [1-6]. It is known that plastic deformation occurs mainly in thin shear bands, and a sharp drop in viscosity in the deformation zones facilitates the propagation of existing shear bands, resulting in the final catastrophic failure of BMGs [1,7]. Macroscopically, the initiation and propagation of shear bands are manifested in serrated plastic flow in the stress-strain curves [8-11]. The serrated flow can be characterised as repeating cycles of elastic loading and unloading, where the loading can be classified as elastic deformation, and the unloading is caused by the inelastic displacement from localized shear band propagation [8-12]. In order to increase the plasticity of a material, the nucleation of the shear bands must be encouraged and the propagation inhibited to avoid catastrophic failure of the shear bands, i.e. the sudden drop of load in the flow serrations [13].

Over the years, geometric confinement has been proven effective in improving the plasticity of BMGs [14-18]. For example, by electroplating a single coating layer of Ni, the plasticity of a nominally "brittle" Fe-based BMG has been increased from 0.5% to 5% [16]. In 2012, Chen at al. [17] reported an improvement in plasticity of a Zr-based BMG using a Cu/Ni bilayer coating, in which the soft Cu coating absorbs the loading stress while the hard Ni layer imposes a confining effect. The bilayer

coating has successfully increased the plasticity of the as-cast Zr-based BMG from 1.3% to 11.2% [17]. The tradeoff, however, turns out to be a significant drop in plastic flow stress upon reaching 7% macroscopic plasticity. Similar phenomena can also be found in single Ni or Cu layer confined BMGs [17].

In a recent work, by applying a MG/Ti bilayer on a Zr-based BMG, Chu et al. have managed to increase the bending plasticity of an uncoated BMG significantly as compared with either uncoated, single MG coated or single Ti coated BMGs [19]. It was shown that the bilayer is capable of absorbing the deformation by initiating a large number of tiny shear bands, which may provide a possible way to further suppress the propagation of shear bands in BMGs in order to achieve more stable plastic flow [19]. In the present study, an amorphous Fe-Ni-W/Ni bilayer has been successfully electroplated on a Zr-based BMG, and more stable plastic flow has been achieved.

2. Experimental

As-cast $Zr_{57}Cu_{20}Al_{10}Ni_8Ti_5$ (at.%) BMG specimens of 2 mm diameter were prepared by sucking the arc melted mixture of high purity raw materials into a copper mould. The electronic plating of the amorphous Fe-Ni-W coating on the BMGs was first carried out using an electrolyte of composition shown in Table I, as modified from Ref. [20]. The pH value of the electrolyte was kept at 8, with the current set at 50 mA for 24 hours. The amorphous nature of the as-cast BMG specimen and the Fe-Ni-W coating was confirmed using an X-ray diffractometer (XRD), and the composition of the amorphous Fe-Ni-W coating was examined using an energy-dispersive X-ray spectrometer (EDS). After the Fe-Ni-W layer plating, a nickel layer was electroplated

onto the existing Fe-Ni-W layer using Watt's electrolyte, containing nickel sulfate, nickel chloride and boric acid [21]. The anode and cathode in this step were pure nickel sheet and the MG coated specimen respectively, and the current was set at 30 mA for 3 hours. Both electroplating experiments were carried out at room temperature, and the solution was constantly stirred by a magnetic rod to achieve a homogeneous-electrolyte over the entire electroplating process. The cathode and anode distances were kept constant, at about 30 mm. Compressive tests of both uncoated and coated specimens were conducted at room temperature on a MTS 810 materials testing system at a strain rate of $1x10^{-4}$ s^{-1}, using an extensometer (model 632.13F-20) to measure the strain. The Vickers hardness data of the as-cast BMGs and the amorphous Fe-Ni-W coatings were obtained using a VH5N-B hardness tester.

3. Results and discussion

Figure 1 shows the XRD patterns of the as-cast BMG specimens and the electroplated Fe-Ni-W coatings. The results show two broad peaks, confirming the amorphous nature of the $Zr_{57}Cu_{20}Al_{10}Ni_8Ti_5$ specimens and the Fe-Ni-W coating. The EDS results show that the composition of the amorphous Fe-Ni-W coating is $Fe_{29.23}Ni_{28.90}W_{41.87}$. An optical image of the cross-section of the bilayer confined BMGs is shown in Fig. 2. The thicknesses of the amorphous Fe-Ni-W layer and the Ni layer were found to be 75.28 μm and 20.39 μm, respectively. It can be seen that the bilayer coating has a good appearance and the two layers are embedded together with no visible microcracks in the interface.

Figure 3 illustrates the compressive stress-strain curves for the uncoated and bilayer coated BMGs. When compared with the uncoated BMG, although the bilayer

confined BMG has a relatively smaller yield strength, the macroscopic plasticity has been enhanced from 1.3% to 10.7%. When comparing the results obtained in this experiment with those obtained by Chen *et al*. using a similar Cu/Ni bilayer confined BMG [17], both specimens show similar plasticity, but the current plateau stress level in the amorphous Fe-Ni-W/Ni coated BMG is notably higher than in the Cu/Ni coated BMG. It is obvious that the amorphous Fe-Ni-W/Ni coated specimen has a much wider plastic deformation range with relatively stable plastic flow, and insignificant decrement in the plastic flow stresses as compared with either the as-cast BMG, single Ni or Cu coated BMG or Cu/Ni bilayer coated BMG [17].

It is well known that the stress increase during the plastic flow of BMGs is correlated with the arrest of the propagating shear bands. However, when a shear band is initiated and starts to propagate, there is a corresponding displacement burst, which is linked to the stress decrease [22]. The repeated stress increase and decrease results in serrations as the plastic flow proceeds. Such successive serrations are recognized as arising from the emission of new shear bands and propagation of the existing ones [17]. To obtain detailed information on the serrated flow between the uncoated BMG and the bilayered confined BMGs, five ranges (as indicated by the rectangle in Fig. 3) of the stress-strain curves have been magnified, and are shown in Fig. 4 and Fig. 5 respectively. Since the bilayer confined BMG specimen has much larger plasticity, two plastic ranges have been magnified in Fig. 5. As shown in Fig. 4 and Fig. 5, during the elastic ranges, the stress increases linearly with time, while during the plastic ranges, serrated flows are clearly observed for both kinds of BMG specimen. However, the amplitude of the serrated flow in the bilayer confined BMGs is much smaller compared to that of the uncoated BMG. The serrated flow of the BMGs is

found to be related to the shear band propagation and termination, which dissipates the plastic deformation energy [23,24]. A smaller amplitude indicates that the rapid avalanching of the load in the specimens has been significantly confined [25].

Flow serrations are the result of intermittent sample sliding and the formation of shear bands along the principal shear plane [8,17]. To characterise the flow serrations, an absolute value of the stress raises/drops ($|\Delta\sigma_s| = |\sigma_{n+1}-\sigma_n|$, where σ_{n+1} and σ_n are two neighbouring values of the stresses on the stress-strain curves) has been introduced. Detailed statistical results of the $|\Delta\sigma_s|$ value of the selected ranges in Fig. 4 and Fig. 5 are shown as histograms in Fig. 6 and Fig. 7 respectively. It can be seen that, in the plastic ranges, the uncoated BMG shows a large stress drop of up to 60 MPa (Fig. 6), while the bilayer confined BMG has a relatively smaller stress drop no larger than 35 MPa (Fig. 7). The smaller amplitudes of the stress drops indicate that the specimen has smaller axial displacement during the avalanches [8], and the specimen can more easily self-organize to a critical state to obtain enhanced macroscopic plasticity [25]. Moreover, the number of the stress drops of the bilayer confined BMGs is larger than the uncoated BMG specimen (due to the vibration of the testing machine, only stresses larger than 12 MPa were determined here [25]), illustrating the initiation of more shear bands in the bilayer confined BMGs.

Serrated flow can also be explained as a cycle of elastic energy accumulation (stress raise) and release (stress drop): a larger serration magnitude would correspond to a higher elastic energy density. As discussed earlier, the serrations obtained for the bilayer confined BMG are of small amplitude and larger frequency, and their corresponding elastic energies are not dense enough for the shear bands to propagate

through the cross section of the specimen [9,10]. The large number of small serration flows is a good indicator that the bilayer confined specimen can release the elastic energy in multiple small bursts rather than releasing all the stored energy in one shear band, thus extending the plastic deformation stage in a more stable manner without large decrease of stress.

Several studies have shown that the geometric confinement is able to affect the plastic flow significantly [14-17]. The process of electroplating can bring about residual stress at the interface between the coating and the BMG [26]. During the elastic loading, the mismatch in the Poisson's ratio of the BMG and the coating would lead to a confining stress on the BMG, and the maximum geometrical confining stress after reaching the yield strength can be estimated by $\sigma_{max} = \sigma_y ln(b/a)$ [27], where σ_{max}, σ_y, a and b denote the maximum confining stress, yield strength of the bilayer coating, inner diameter and outer diameter of the specimen respectively. By replacing part of the Ni coatings with amorphous Fe-Ni-W coatings, the large yield strength of the Fe-based BMG enables larger confining stresses on the BMG matrix [28]. Upon loading, the shear bands start propagating on the surface of the uncoated BMG, and deformation occurs through the primary shear band, leading to catastrophic failure. When the bilayer coating is in the place, it serves to inhibit the rapid propagation of single shear bands, causing them to branch out instead [17]. The enlargement of the confined stress is capable of arresting the propagation of the shear bands to avoid catastrophic failure from avalanches, resulting in a stable plastic flow before failure [16,25].

Recently, many studies have reported that the interface can induce the initiation of more smaller shear bands and the corresponding increased interactions (branching and arresting) between the shear bands, which would in turn increase the plasticity of the coated specimen [16,19]. Besides the confining effect, the outside nickel layer is also found to be effective in hindering the propagation of the shear bands in dissipating the stored elastic energy in the core BMG [16]. Moreover, since the hardness of the Fe-Ni-W coatings (measured as 647 HV) is much larger than the hardness of the BMG specimen (about 442 HV), the inner Zr-BMG may act as a softer phase for the initiation of the shear bands, and the outer amorphous Fe-Ni-W layer may act as a harder phase for inhibiting the propagation of the shear bands [29,30]. The complicated mechanisms for the initiation and propagation of the shear bands (intermittent sliding) in the bilayer confined BMGs may need further verification, however, the corresponding serrated flow shown in the stress-strain curves, without much decreasing of the loads, distinctly illustrates stable plastic flow in bilayer confined BMGs. This provides a feasible route for achieving stable plastic flow in BMGs for use in industrial applications and as guidance in understanding the plastic deformation mechanism in geometrical confined BMGs.

4. Conclusions

An amorphous Fe-Ni-W/Ni bilayer has been successfully coated onto a Zr-based BMG through electroplating. The bilayer confined BMG exhibits greatly enhanced macroscopic plasticity till failure, without much decrease of the loads during the serrated flow stage. The statistical results of the flow serrations show that the bilayer confined BMG has smaller amplitudes as well as larger frequencies of stress decreases. The enhanced stability of the plastic flow in bilayer confined BMGs may

be mainly due to the large confining effect brought about by the amorphous layer. The present work not only proposes a feasible route to achieve more stable plastic flow in BMGs but also gives more insight into the plastic deformation mechanisms of geometric confined BMGs.

Acknowledgements

The work described in this paper was supported by a grant from the Research Grants Council of the Hong Kong Special Administrative Region, China (Project No.: PolyU 511510).

References

[1] A. R. Yavari, J. J. Lewandowski, J. Eckert, Mechanical properties of bulk metallic glasses, Mrs Bulletin, 32 (**2007**) 8, 635-638, doi:10.1557/mrs2007.125

[2] W. H. Wang, C. Dong, C. H. Shek, Bulk metallic glasses, Materials Science and Engineering R, 44 (**2004**) 2-3, 45-89, doi:10.1016/j.mser.2004.03.001

[3] A. L. Greer, Metallic glasses ... on the threshold, Materials Today, 12 (**2009**) 1-2, 14-22, doi:10.1016/S1369-7021(09)70037-9

[4] S. H. Chen, K. C. Chan, F. F. Wu, L. Xia, Pronounced energy absorption capacity of cellular bulk metallic glasses, Applied Physics Letters, 104 (**2014**) 11, 111907, doi: 10.1063/1.4869229

[5] S. H. Chen, K. C. Chan, L. Xia, Deformation behavior of a Zr-based bulk metallic glass under a complex stress state, Intermetallics, 43 (**2013**), 38-44, doi: 10.1016/j.intermet.2013.07.006

[6] S. H. Chen, K. C. Chan, L. Xia, Deformation behavior of bulk metallic glass structural elements, Materials Science and Engineering A, 606 (**2014**), 196-204, doi: 10.1016/j.msea.2014.03.094

[7] A. S. Argon, Plastic-Deformation in Metallic Glasses, Acta Metallurgica, 27 (**1979**) 1, 47-58, doi:10.1016/0001-6160(79)90055-5

[8] S. X. Song, H. Bei, J. Wadsworth, T. G. Nieh, Flow serration in a Zr-based bulk metallic glass in compression at low strain rates, Intermetallics, 16 (**2008**) 6, 813-818, doi:10.1016/j.intermet.2008.03.007

[9] C. N. Kuo, H. M. Chen, X. H. Du, J. C. Huang, Flow serrations and fracture morphologies of Cu-based bulk metallic glasses in energy release perspective, Intermetallics, 18 (**2010**) 8, 1648-1652, doi:10.1016/j.intermet.2010.04.018

[10] J. W. Qiao, Y. Zhang, P. K. Liaw, Serrated flow kinetics in a Zr-based bulk metallic glass, Intermetallics, 18 (**2010**) 11, 2057-2064, doi: 10.1016/j.intermet.2010.06.013

[11] S. X. Song, T. G. Nieh, Flow serration and shear-band viscosity during inhomogeneous deformation of a Zr-based bulk metallic glass, Intermetallics, 17 (**2009**) 9, 762-767, doi:10.1016/j.intermet.2009.03.005

[12] W. J. Wright, R. Saha, W. D. Nix, Deformation mechanisms of the $Zr_{40}Ti_{14}Ni_{10}Cu_{12}Be_{24}$ bulk metallic glass, Materials Transactions, 42 (**2001**) 4, 642-649, doi:10.2320/matertrans.42.642

[13] B. A. Sun, S. Pauly, J. Tan, M. Stoica, W. H. Wang, U. Kuhn, J. Eckert, Serrated flow and stick-slip deformation dynamics in the presence of shear-band interactions for a Zr-based metallic glass, Acta Materialia, 60 (**2012**) 10, 4160-4171, doi:10.1016/j.actamat.2012.04.013

[14] H. Q. Li, L. Li, C. Fan, H. Choo, P. K. Liaw, Nanocrystalline coating enhanced ductility in a Zr-based bulk metallic glass, Journal of Materials Research, 22 (**2007**) 2, 508-513, doi:10.1557/Jmr.2007.0060

[15] W. Chen, K. C. Chan, P. Yu, G. Wang, Encapsulated Zr-based bulk metallic glass with large plasticity, Materials Science and Engineering A, 528 (**2011**) 6, 2988-2994, doi:10.1016/j.msea.2010.12.077

[16] W. Chen, K. C. Chan, S. F. Guo, P. Yu, Plasticity improvement of an Fe-based bulk metallic glass by geometric confinement, Materials Letters, 65 (**2011**) 8, 1172-1175, doi:10.1016/j.matlet.2011.01.030

[17] W. Chen, K. C. Chan, S. H. Chen, S. F. Guo, W. H. Li, G. Wang, Plasticity enhancement of a Zr-based bulk metallic glass by an electroplated Cu/Ni bilayered coating, Materials Science and Engineering A, 552 (**2012**), 199-203, doi:10.1016/j.msea.2012.05.031

[18] T. G. Nieh, Y. Yang, J. Lu, C. T. Liu, Effect of surface modifications on shear banding and plasticity in metallic glasses: An overview, Progress in Natural Science: Materials International, 22 (**2012**) 5, 355-363, doi:10.1016/j.pnsc.2012.09.006

[19] J. P. Chu, J. E. Greene, J. S. C. Jang, J. C. Huang, Y. L. Shen, P. K. Liaw, Y. Yokoyama, A. Inoue, T. G. Nieh, Bendable bulk metallic glass: Effects of a thin, adhesive, strong, and ductile coating, Acta Materialia, 60 (**2012**) 6-7, 3226-3238, doi:10.1016/j.actamat.2012.02.037

[20] F. J. He, J. Yang, T. X. Lei, C.Y. Gu, Structure and properties of electrodeposited Fe-Ni-W alloys with different levels of tungsten content: A comparative study, Applied Surface Science, 253 (**2007**) 18, 7591-7598, doi:10.1016/j.apsusc.2007.03.068

[21] L. Mirkova, G. Maurin, M. Monev, C. Tsvetkova, Hydrogen coevolution and permeation in nickel electroplating, Journal of Applied Electrochemistry, 33 (**2003**) 1, 93-100, doi:10.1023/A:1022957600970

[22] H. M. Chen, C. J. Lee, J. C. Huang, T. H. Li, J. S. C. Jang, Flow serration and shear-band propagation in porous Mo particles reinforced Mg-based bulk metallic glass composites, Intermetallics, 18 (**2010**) 6, 1240-1243, doi:10.1016/j.intermet.2010.03.024 (2010)

[23] A. Lemaitre, C. Caroli, Rate-Dependent Avalanche Size in Athermally Sheared Amorphous Solids, Physical Review Letters, 103 (**2009**) 6, 065501, doi:10.1103/Physrevlett.103.065501

[24] D. Klaumunzer, R. Maass, F. H. Dalla Torre, J. F. Loffler, Temperature-dependent shear band dynamics in a Zr-based bulk metallic glass, Applied Physics Letters, 96 (**2010**) 6, 061901, doi:10.1063/1.3309686

[25] G. Wang, K. C. Chan, L. Xia, P. Yu, J. Shen, W. H. Wang, Self-organized intermittent plastic flow in bulk metallic glasses, Acta Materialia, 57 (**2009**) 20, 6146-6155, doi:10.1016/j.actamat.2009.08.040

[26] S. J. Hearne, J. A. Floro, Mechanisms inducing compressive stress during electrodeposition of Ni, Journal of Applied Physics, 97 (**2005**) 1, 014901, doi:10.1063/1.1819972

[27] G. Ravichandran, J. Lu, Pressure-dependent flow behavior of $Zr_{41.2}Ti_{13.8}Cu_{12.5}Ni_{10}Be_{22.5}$ bulk metallic glass, Journal of Materials Research, 18 (**2003**) 9, 2039-2049, doi:10.1557/Jmr.2003.0287

[28] X. J. Gu, S. J. Poon, G. J. Shiflet, Mechanical properties of iron-based bulk metallic glasses, Journal of Materials Research, 22 (**2007**) 2, 344-351, doi:10.1557/Jmr.2007.0036

[29] X. H. Du, J. C. Huang, K. C. Hsieh, Y. H. Lai, H. M. Chen, J. S. C. Jang, P. K. Liaw, Two-glassy-phase bulk metallic glass with remarkable plasticity, Applied Physics Letters, 91 (**2007**) 13, 131901, doi:10.1063/1.2790380

[30] S. H. Chen, K. C. Chan, L. Xia, Effect of stress gradient on the deformation behavior of a bulk metallic glass under uniaxial tension, Materials Science and Engineering A, 574 (**2013**), 262-265, doi:10.1016/j.msea.2013.03.035

Table captions

Table I Electrolyte composition for amorphous Fe-Ni-W layer deposition.

Component	**Concentration/ mol L^{-3}**
Iron Sulfate	0.20
Nickel Sulfate	0.05
Sodium Tungstate	0.13
Citric Acid	0.29

Figure captions

Figure 1. XRD patterns of the $Zr_{57}Cu_{20}Al_{10}Ni_8Ti_5$ BMG and the amorphous Fe-Ni-W coating.

Figure 2. Optical image of the amorphous Fe-Ni-W/Ni bilayer coated BMG.

Figure 3. Compressive stress-strain curves for the uncoated and bilayer coated BMG specimens.

Figure 4. Flow serrations of the uncoated BMG.

Figure 5. Flow serrations of the bilayer coated BMG.

Figure 6. Statistical results of the number of stress loads/drops for the uncoated BMG.

Figure 7. Statistical results of the number of stress loads/drops for the bilayer confined BMG.

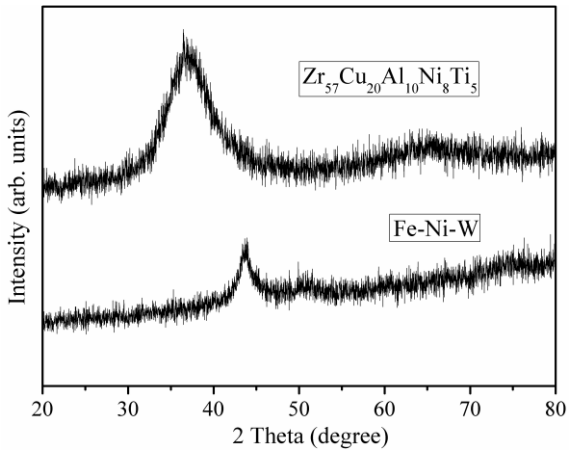

H.Q. Lau *et al.*

Figure 1

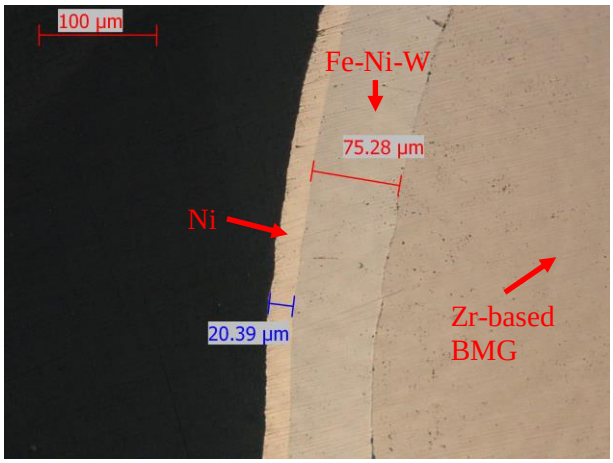

H.Q. Lau *et al.*

Figure 2

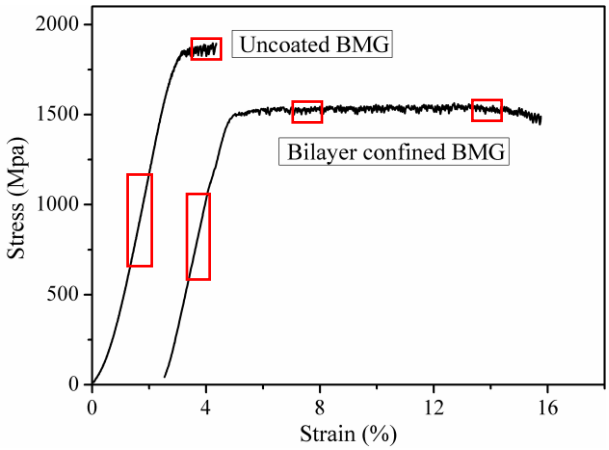

H.Q. Lau *et al.*

Figure 3

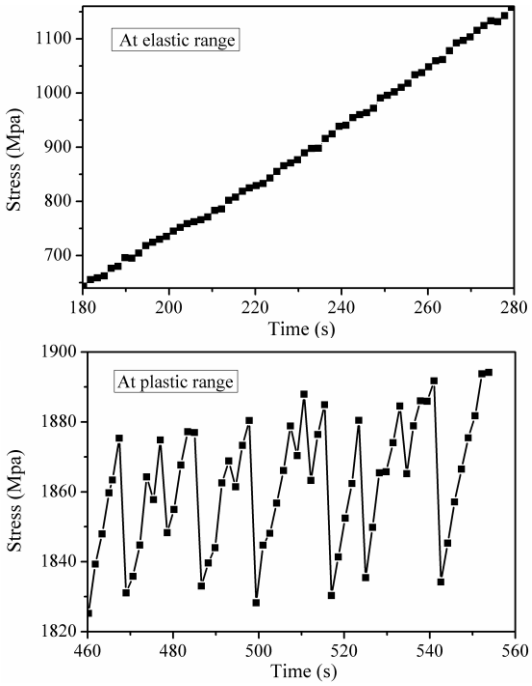

H.Q. Lau *et al.*

Figure 4

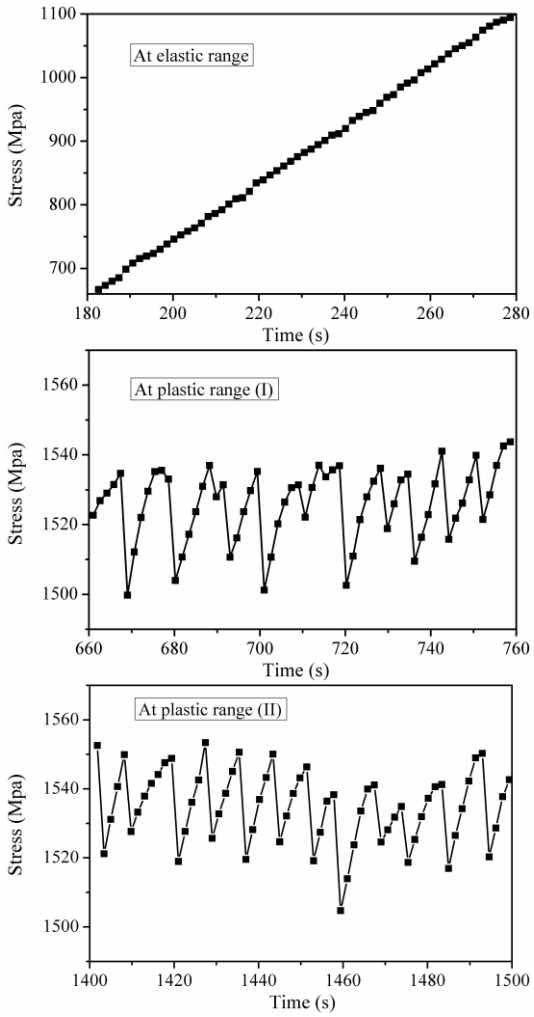

H.Q. Lau *et al.*

Figure 5

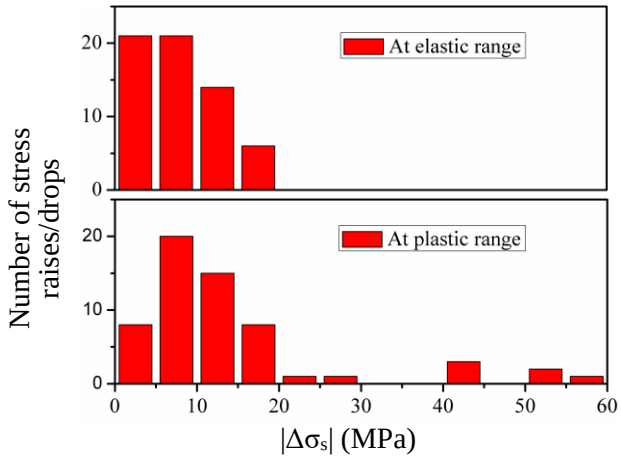

H.Q. Lau *et al.*

Figure 6

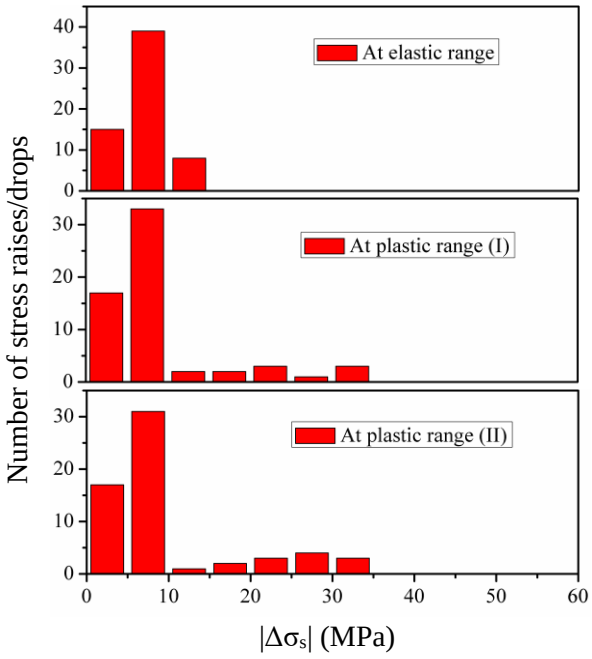

H.Q. Lau *et al.*

Figure 7